Assessment of Land Use Land Cover Changes and Future Predictions Using CA-ANN Simulation for Selangor, Malaysia

Mohammed Feras Baig [1,*], Muhammad Raza Ul Mustafa [1,2,*], Imran Baig [3], Husna Binti Takaijudin [1,2] and Muhammad Talha Zeshan [1]

[1] Department of Civil and Environmental Engineering, Universiti Teknologi PETRONAS, Seri Iskandar 32610, Perak, Malaysia; husna_takaijudin@utp.edu.my (H.B.T.); talhaansari510@gmail.com (M.T.Z.)

[2] Centre for Urban Resource Sustainability, Institute of Self-Sustainable Building, Universiti Teknologi PETRONAS, Seri Iskandar 32610, Perak, Malaysia

[3] Department of Electrical and Computer Engineering, College of Engineering, Dhofar University, Salalah 211, Oman; ibaig@du.edu.om

* Correspondence: Feras_19001701@utp.edu.my (M.F.B.); raza.mustafa@utp.edu.my (M.R.U.M.)

Abstract: Land use land cover (LULC) has altered dramatically because of anthropogenic activities, particularly in places where climate change and population growth are severe. The geographic information system (GIS) and remote sensing are widely used techniques for monitoring LULC changes. This study aimed to assess the LULC changes and predict future trends in Selangor, Malaysia. The satellite images from 1991–2021 were classified to develop LULC maps using support vector machine (SVM) classification in ArcGIS. The image classification was based on six different LULC classes, i.e., (i) water, (ii) developed, (iii) barren, (iv) forest, (v) agriculture, and (vi) wetlands. The resulting LULC maps illustrated the area changes from 1991 to 2021 in different classes, where developed, barren, and water lands increased by 15.54%, 1.95%, and 0.53%, respectively. However, agricultural, forest, and wetlands decreased by 3.07%, 14.01%, and 0.94%, respectively. The cellular automata-artificial neural network (CA-ANN) technique was used to predict the LULC changes from 2031–2051. The percentage of correctness for the simulation was 82.43%, and overall kappa value was 0.72. The prediction maps from 2031–2051 illustrated decreasing trends in (i) agricultural by 3.73%, (ii) forest by 1.09%, (iii) barren by 0.21%, (iv) wetlands by 0.06%, and (v) water by 0.04% and increasing trends in (vi) developed by 5.12%. The outcomes of this study provide crucial knowledge that may help in developing future sustainable planning and management, as well as assist authorities in making informed decisions to improve environmental and ecological conditions.

Keywords: land use land cover (LULC); support vector machine (SVM); cellular automata-artificial neural network (CA-ANN); change detection; sustainable development

1. Introduction

Humans have made major modifications to the earth's surface over time in order to generate food via farming methods. Over half of the earth's surface has been transformed in the last few years [1], and over one-third of the earth's surface is believed to be agricultural. This process of transitioning from naturally occurring farming land to agricultural land is still currently ongoing [2]. Land use administrators and experts have been investigating the impact of land use changes on hydrological processes as a result of these major changes [3]. Analyzing patterns in change detection, land use managers, and decision makers may gain a better understanding of the relationships between human and natural processes. According to [4], the massive increase in population is the most important element in the global shift of land use.

The transition of natural regions into industrial or agricultural fields is mainly responsible for the dramatic differences in land cover, especially in developing nations [5]. The hydrological cycle and river basin processes are under significant stress as natural land,

dense forests, and watersheds are diminished [6]. Land use and water quality changes can be influenced by anthropogenic activities, such as industrialization, urbanization, and mining [7,8]. These patterns of LULC are thought to have a substantial impact on groundwater quality [9,10]. The US Geological Survey (USGS) investigated the impact of changing land conditions on local groundwater quality to establish a correlation between the LULC and groundwater quality in 1984. He et al., [11] illustrates the effects of different types of land use on groundwater quality by establishing that carcinogenic risks caused by Cr6+ were related to urban lands and exposure to NO3− and Cr6+ related to agricultural lands created non-carcinogenic risks. Nitrate concentrations in groundwater are also linked to paved light-duty roads [12]. Change detection is a method for identifying changes in any process or resource by analyzing data over several time periods [13]. For the evaluation of changes in the spatial features of the land, it is critical to offer multi-temporal datasets [14]. The use of multi-temporal datasets simplifies the understanding of significant LULC shifts and trends [15]. The launch of Landsat satellites and improvements in computer technology have made it easier to trace the changes and advancements that have happened over the past decades.

The use of remote sensing technology in conjunction with a geographic information system (GIS) has proven to be effective in identifying a variety of environmental characteristics, such as vegetation cover, urban sprawls, forest changes, and, particularly, variations in LULC changes over time [16]. In comparison to other conventional methods and surveys, remote sensing and GIS techniques have shown to provide more reliable and cost-effective data assessments [5]. Remote sensing is described as the monitoring of spatial changes in various elements without interacting with them physically. Remote sensing uses space-based satellites to classify the earth's unique attributes, which can aid in tracking changes on the land surface since they monitor the earth's characteristics on a regular basis [17]. Scientists and researchers can detect large-scale changes in land use patterns with the knowledge acquired on a temporal and spatial level, allowing regional politicians and authorities to make future decisions. Many studies have documented the use of remote sensing in natural disaster management. For example, it has been used in India to monitor floods [18]. Alexakis et al., [19] investigated geomorphic variables in order to develop a decision support system to prevent landslides using remote sensing. It has also been helpful in detecting changes in agricultural patterns, land cover changes, and urban sprawl [20]. For detecting changes in remotely sensed data, GIS is considered a vital tool [21]. It allows for the integration of data from many sources in order to detect changes. The combined effect of hydrological data, soil, topographic maps, and classified images produced by GIS may be useful in extracting land use information for a particular region. Furthermore, because of its flexibility to create the model using the supplied statistics and information, it may be able to illustrate trends in land use changes. Furthermore, GIS and remotely sensed data are often used to detect LULC changes [22]. The combined use of GIS and remote sensing has been shown to be a viable and effective approach for tracking land cover changes [23]. Many works [24,25] have proven the effectiveness of space-borne imaging in mapping LULC changes. Gammal et al., [26] utilized many Landsat data from several time periods (1972–2008) to examine land use and land cover changes in Egypt. Landsat images over several years were utilized to evaluate LULC trends in Rwanda [27]. Similarly, several studies in Malaysia have been published to track LULC patterns in various regions [28]. LULC changes were observed in parts of the Cameron Highlands by implementing SVM image classification [29]. Al-Najjar et al. [30] assessed the LULC changes using convolutional neural networks on DSM and UAV images. The transitions and change detection techniques are revealed using conventional approaches for assessing the spatiotemporal extent of LULC changes.

Parametric and non-parametric classifiers are the two types of classification techniques. Parametric classifiers presume that the data for each class is regularly distributed [31]. The maximum likelihood classification (MLC) is the most extensively used parametric classifier, which generates decision surfaces based on the mean and covariance of each class [32,33].

Non-parametric image classification approaches, such as the artificial neural network (ANN) and the support vector machine (SVM), make no assumptions about the statistical character of the data and are relatively new image classification techniques. SVM is a non-parametric classifier that consists of a collection of linked learning algorithms that may be used for classification and regression [34,35]. Machine-learning techniques, such as artificial neural networks (ANNs), the SVM, Random Forest, decision tree, and other models, have garnered considerable attention for LULC classification [36–39]. The level of accuracy for each machine-learning approach is different. ANN, SVM, and Random Forest have been reported to have higher accuracy than other conventional classifier methods [40], and SVM and Random Forest are the best approach for LULC classification when compared to all other machine-learning techniques [41,42].

Land use planners, resource managers, and conservation officers can utilize predicted LULC changes to promote sustainable land management and mitigate adverse consequences. As a result, LULC change detection and prediction have become essential considerations in a wide array of disciplines, such as identifying biodiversity hotspots for prioritizing conservation efforts, modelling rural and urban planning [43,44], and investigating degradation processes, among others [45]. Aerial imagery and historical maps have been used in conjunction with geospatial technologies and remote sensing to characterize landscape dynamics and deliver scientifically reliable results and action plans that have aided policymakers and planners in advancing sustainable development, particularly in rapidly growing urban environments [46]. As a result, transition potential modelling and projecting future LULC under the impact of geographical factors are used to figure out where changes have occurred and may occur in the future [47]. Most of these models analyze LULC transitions using temporal land-use data, which, combined with spatial factors, may forecast future LULC possibilities [48]. A variety of models have been developed so far for forecasting and simulating LULC changes [49]. Statistical-based techniques and machine learning methods have also been utilized for decades in land use modelling [34,50]. To analyze the LULC change process, researchers often utilize a combination of models, GIS, and remote sensing methods. Models based on equations [42], statistics [35], Markov chains [28], and cellular models are the most used approaches.

Selangor is the economic hub of Malaysia due to its location and proximity to the countries capital, as well as its developed transportation system. The rapid urbanization and industrialization can prove to be a challenge for sustainability of the region. The study aims to observe the land use changes in the years 1991, 2001, 2011, and 2021 within the region of Selangor. The study will also focus on identifying the driving force for the LULC changes. CA-ANN simulation was also conducted to analyze the predicted land use patterns and trends from 2031 to 2051. Previous studies showed several concerns related to data quality, data inconsistency, data harmonization, validation of data, and uncertainties linked with data [51]. It has also appeared from literature that no study has been conducted to investigate LULC pattern changes and prediction in Selangor state. Additionally, the land use classification in previous studies was conducted by a parametric method of classification, resulting in lower accuracy of classification that also affected the prediction results. However, the SVM classification method was used in this study to obtain higher accuracy of land use classification and prediction. The results can provide valuable hints to regional authorities for future decisions.

2. Materials and Methods

2.1. Study Area

The study area considered for this study was the state of Selangor, Malaysia. Selangor is Malaysia's most developed and densely inhabited state. The state of Selangor is divided into nine districts, as shown in Figure 1. Selangor is located on the western cost of Malaysia. The state is surrounded by the state of Perak to the north, state of Negeri Sembilan to its south, and the state of Pahang to its east. The study area was located between the latitudes ranging from $2°35'$ to $3°60'$ N and longitudes ranging from $100°45'$ to $102°00'$ E. The total

area of Selangor is 8100 Km^2 with the population of over 6.5 million. The temperature in Selangor ranges between 23 to 30 °C, with an annual mean temperature of 26 °C. Selangor experiences sunny days throughout most of the year, with sporadic rainfall. The annual rainfall in Selangor is 1200 mm, and humidity reaches more than 80% [46]. Kuala Lumpur, the capital of the country, and the federal administrative capital, Putrajaya, are located within the state of Selangor and were considered in the study area. Of all Malaysian states, Selangor has the greatest population density and gross domestic output per capita. Selangor is geographically diverse, having major metropolitan centers, agricultural development, forests, and wetlands, as well as a wide range of land use and related environmental aspects [47].
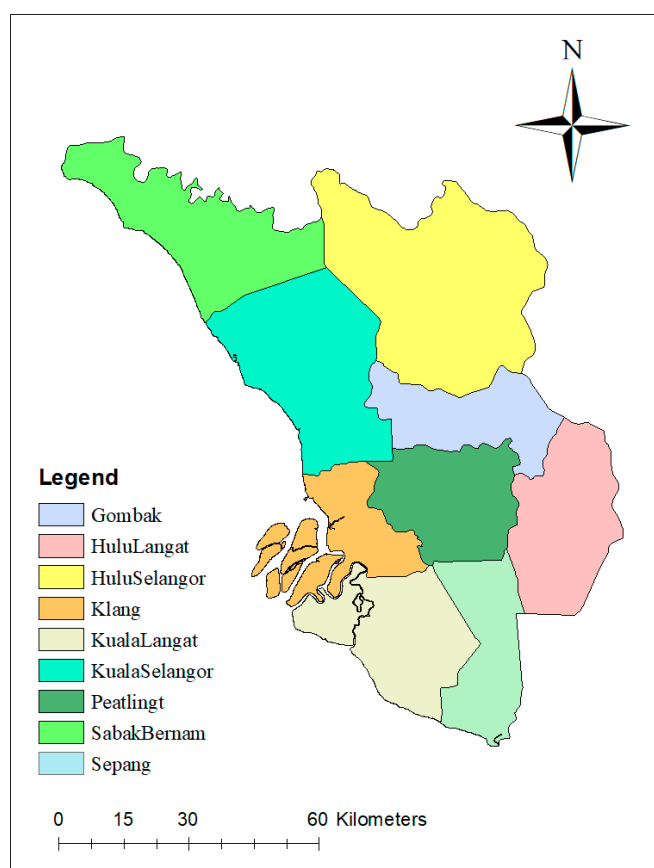
Figure 1. Study area map of Selangor, Malaysia.

2.2. Data Collection and Processing

The Landsat images for the years 1991, 2001, 2011, and 2021 were used for image classification to identify land use patterns and create LULC maps. Landsat-5 satellite images were obtained for 1991 and 2001. Similarly, Landsat-8 satellite images were acquired for 2011 and 2021. The Landsat images had the spatial resolution for 30 m. Images with cloud cover of less than 5% were only selected to maintain quality and uniform weather conditions throughout the study period. The Landsat images were acquired from USGS through their earth explorer web portal (https://glovis.usgs.gov/ (Retrieved on 21 October 2021). The satellite images were analyzed and processed (geo-referencing, mosaic, and extraction) to correct its geospatial imagery. Multiple band combinations were used to identify the land use patterns within the Landsat images. Visible bands (red, green, and blue) 3, 4, and 5 were used for Landsat-5 images, and bands 4, 5, and 6 were used for Landsat-8 images. Landsat images were spatially projected to WGS_1984_UTM_Zone_49N. The study area of Selangor was then extracted from the projected datasets to create a raster for image classification. The digital elevation model (DEM) was also obtained from the

USGS web portal, which was analyzed using ArcGIS to create spatial maps, such as slope and aspect. The data for transportation and road networks was downloaded from Diva-GIS (https://www.diva-gis.org/ (Retrieved on 21 October 2021)). ArcGIS was employed to find the distance from major roads using the Euclidean distance method. Figure 2 shows the spatial parameters used for predicting the land use changes. Google Earth and public map datasets were also utilized for reference and better understanding of land use distribution.
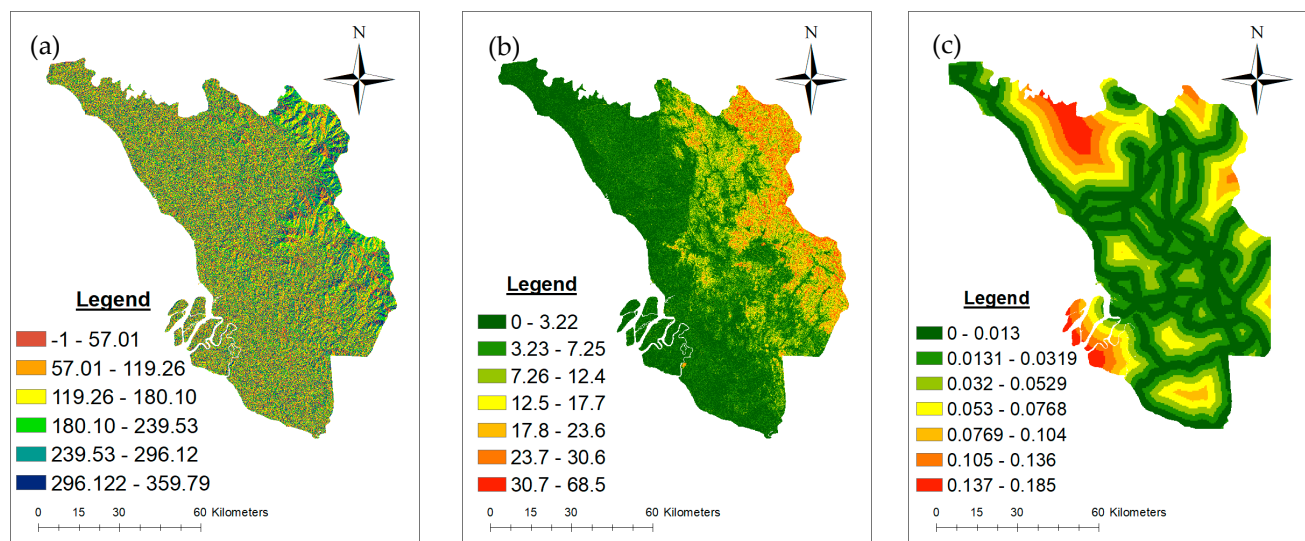
Figure 2. Spatial parameter map of Selangor, Malaysia. (**a**) Aspect, (**b**) slope, (**c**) distance from road.

2.3. Land Use Classification and Accuracy Assessment

The land use classification of satellite images was done by implementing a pixel-based, supervised classification technique. Upon analysis of the study area, six different land use classes were identified: (a) water, (ii) developed, (iii) barren, (iv) forest, (v) agricultural, and (vi) wetlands. Based on the LULC classes, training samples were collected using defined polygons upon the various locations of different land use classes. A suitable spectral signature helps to guarantee that there is little misunderstanding between the land covers to be mapped [48]. The collected training samples were grouped depending on the land cover. A total of 30 training samples were collected for each of the six land use classes considered for image classification. The signature file was then created as the training dataset for the purpose of supervised classification. The land use classification was done via the support vector machine (SVM) algorithm. Although SVM is primarily developed for binary classification, it may also be used to identify patterns and objects, and it can be used for both pixel-based and object-based classifications [34]. The SVM does not require a large number of ground truth samples for training and does not assume that the data are selected from a specific probability distribution [42]. Using a feature vector and model parameters, the SVM seeks to identify the best hyperplane that defines the class boundary during the training phase [35]. Only the samples in the margin between classes are utilized to create the optimum hyperplane in the SVM, and they are referred to as support vectors [34]. The flow chart illustrating the process for land use classification to create LULC maps is shown in Figure 3.

The accuracy of classified maps was assessed by comparing the created land use maps for 1991, 2001, 2011, and 2021, with the referenced satellite imagery and public land use maps for the state of Selangor. To enhance accuracy, the output classification results were visually inspected multiple times before being updated by introducing new training sets. In order to compute the accuracy of the classified thematic maps, sample points were randomly distributed on the classified maps using GIS. High resolution images were observed and cross-referenced to determine the ground truth of the selected sample points. Each point position was analyzed based on the polygon into which it was placed and

compared to the reference image to determine whether or not it was accurately identified. These sample points were then converted into a confusion matrix. The confusion matrix was used to determine the kappa coefficient [52], overall accuracies, and user and producer accuracies [53].
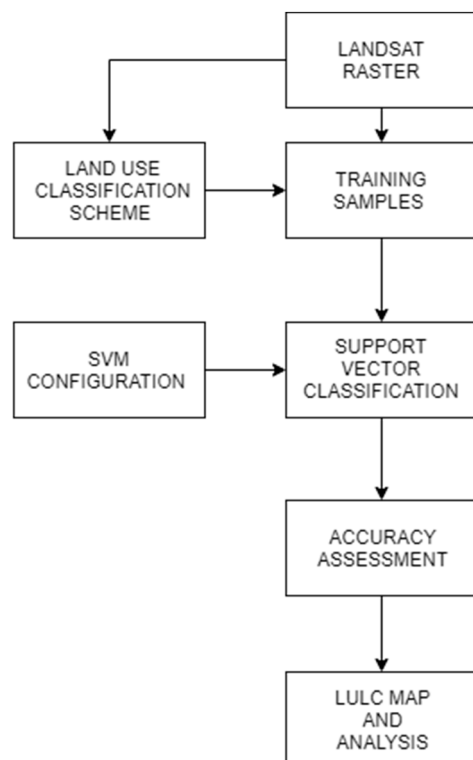
Figure 3. Flow chart for creating LULC maps using SVM image classification.

2.4. Cellular Automata-Artificial Neural Network Simulation

Simulation modules were used to minimize the dynamics of composite urban structures and interpret them in a clear and accessible manner. Studies claim that the CA-ANN method is more effective than linear regression, thus the modules for the land-use change simulation (MOULSCE) plugin were implemented for transition potential modelling and future simulation [54,55]. The MOLUSCE plugin is perfectly adapted to evaluating spatiotemporal land-use changes, transition potential modelling, and predicting future scenarios [54]. The artificial neural network (ANN) was used in association with cellular automata (CA) to predict the land use changes. Because of its dynamic simulation capacity, high efficiency with limited data, simple calibration, and ability to reproduce different land covers and complicated patterns, CA-ANN was chosen to simulate land use change. CA-ANN combines the CA and Markov chain to model land use changes across various categories [56]. ANN was employed in the transition potential modelling to establish trends on the basis of which future prediction will be made. The MOLUSCE plugin within QGIS was executed to establish the spatiotemporal changes with a given time period and calculate the LULC transition to generate the LULC change map. A transition potential matrix was generated in the study between (2001–2011) to create the change map. The ANN-multilayer perception method (ANN-MLP) was employed for the transition potential modelling. Slope, aspect, elevation, and distance from the road were the spatial parameters implemented as input parameters. The structure of ANN-MLP is shown in Figure 4, where the input layer is processed by the hidden layers and produces the output layer containing the reclassified LULC classes. The transition potential model is trained based on the LULC maps of 2001 and 2011, as well as spatial parameters to produce the predicted map of 2021.
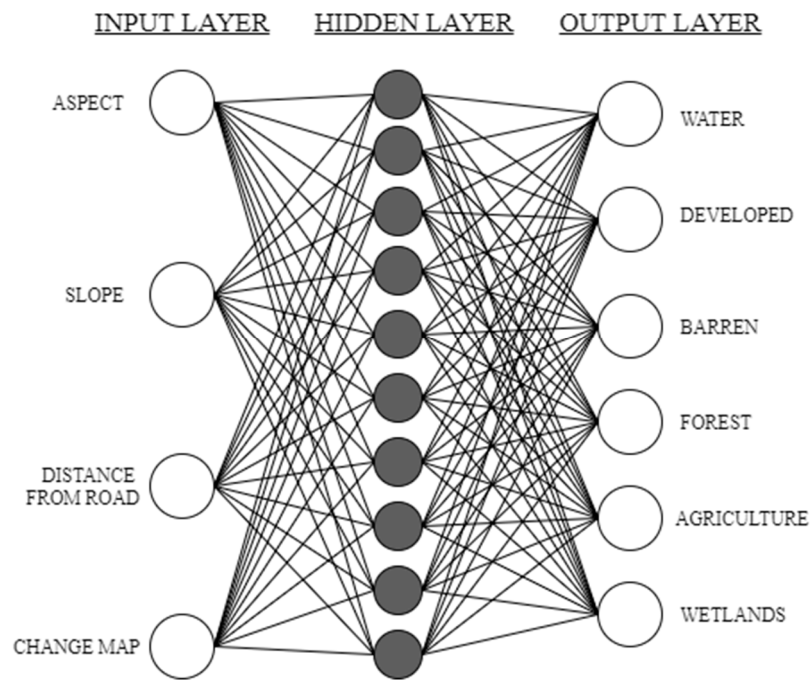
Figure 4. Structure of ANN-MLP model used for predicting the land use transition potential.

In order to validate the ANN model, the simulated map of 2021 was compared with the classified LULC map of 2021. Satisfactory results were obtained, and the model was trained with a learning rate of 0.001 and momentum of 0.001. The ANN training process ran for 100 iteration and a neighborhood value of 3 pixels with 10 hidden layers. The trained model was then simulated to obtain the predicted maps of 2031, 2041, and 2051. The steps of the CA-ANN model are illustrated in Figure 5.
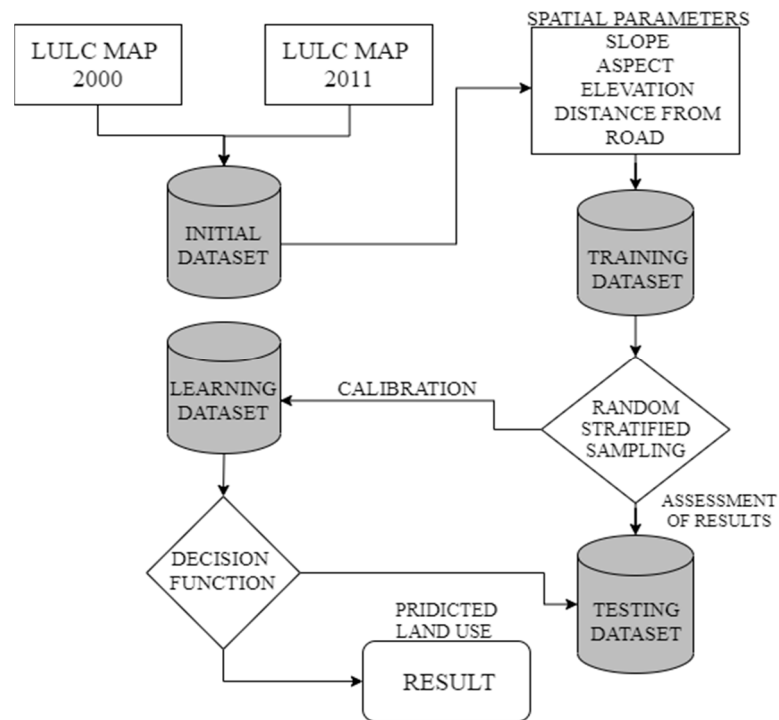
Figure 5. Flow chart illustrating the steps of CA-ANN simulation to predict LULC maps.

3. Results and Discussion

3.1. Land Use and Land Cover Changes in Selangor from 1991 to 2021

The classified LULC maps of the study area for 1991 to 2021 were classified into six different land use classes, namely (i) water, (ii) developed, (iii) barren, (iv) forest, (v) agriculture, and (vi) wetlands. LULC changes were observed over the period of 3 decades, ranging from 1991 to 2001, 2001 to 2011, and 2011 to 2021. Agricultural, forest, and developed areas were found to be the major land use types that cover Selangor, Malaysia, as shown in Figure 6.
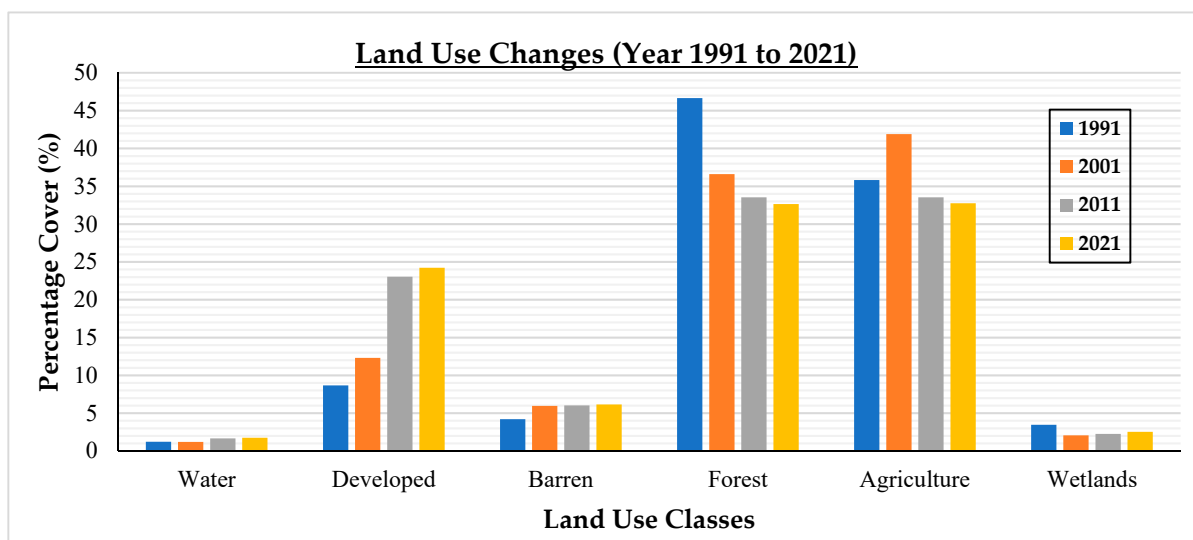
Figure 6. Changes in different land use classes from the year 1991 to 2021 in Selangor.

The distribution of total area covered by the different LULC classes and their percentage of cover in the years 1991, 2001, 2011, and 2021 is shown in Table 1. Agricultural areas experienced a rapid growth from 1991 to 2001, where it increased from 2921.91 Km^2 to 3416.77 Km^2 (35.82% to 41.88%). Between the years 2001 and 2011, agricultural areas experienced a decline in total area coverage as they reduced from 3416.77 Km^2 in 2001 to 2735.24 Km^2 in 2011. In the year 2021, agricultural areas continued their decreasing trend, occupying 2671.36 Km^2 (32.64%) of the total study area. On the other hand, forest covers experienced a drop in percentage cover from 46.65% to 36.59% (3805.57 Km^2 to 2985.31 Km^2) between the years of 1991 and 2001, respectively. A steady decrease in forest covers continued in the years 2011 and 2021 as the area covered was 2734.60 Km^2 and 2662.41 Km^2 (33.52% and 32.64%), respectively. In contrast, developed areas experienced an exponential growth over the observed period. The developed area grew from 707.32 Km^2 (8.67%) in 1991 to 1003.50 Km^2 (12.30%) in 2001. Between the years 2001 and 2011, developed areas had a major expansion as the total area cover in the year 2011 increased to 1878.31 Km^2 (23.02%) and subsequently increased to 1974.95 Km^2 (24.21%) in 2021. Minimal changes were observed in the land use classes of water, barren, and wetlands. Wetlands in the study area reduced from 281.95 Km^2 in 1991 to 168.66 Km^2 in 2001, followed by a rise in 2011 to 183.29 Km^2 and then to 205.40 Km^2 in 2021. The percentage cover of barren lands showed an increase from 4.19% to 5.96% within 1991 and 2001 and then observed minimal change between 2011 and 2021, as the percentage cover was 6.02% and 6.15%, respectively. Water had marginal area changes, where an increasing trend was noted as the total area cover inflated from 99.14 Km^2 in 1991 to 142.49 Km^2 in 2021.

Table 1. Total area cover by different LULC classes and the percentage of cover for the years 1991, 2001, 2011, and 2021 in Selangor.

Years LULC Classes	1991 Area (Km^2)	%	2001 Area (Km^2)	%	2011 Area (Km^2)	%	2021 Area (Km^2)	%
Water	99.14	1.22	97.74	1.20	135.58	1.66	142.49	1.75
Developed	707.32	8.67	1003.50	12.30	1878.31	23.02	1974.95	24.21
Barren	342.11	4.19	486.02	5.96	490.97	6.02	501.40	6.15
Forest	3805.57	46.65	2985.31	36.59	2734.60	33.52	2662.41	32.64
Agriculture	2921.91	35.82	3416.77	41.88	2735.24	33.53	2671.36	32.75
Wetlands	281.95	3.46	168.66	2.07	183.29	2.25	205.40	2.52

The LULC maps of Selangor from the year 1991 to 2021 are shown in Figure 7. The changes in the LULC of Selangor was observed between three periods, from 1991–2001, 2001–2011, and 2011–2021. Table 2 illustrates the changes experienced by each LULC class in terms of area over the three study periods. It was noted from 1991–2001 that forest cover decreased dramatically in covered area, which was attributed to agricultural lands taking over forest lands. Due to this conversion, agricultural lands saw great expansion, accompanied by significant changes in barren lands. Wetlands were also affected as the area covered sustained a major drop. In the 2001–2011 period, a rapid growth was noted in the total area covered by developed lands. This exponential rise was at the cost of agricultural areas as the area covered by agricultural lands reduced significantly. Forest cover continued to decrease but at a slower rate compared to the previous period. Since forest lands, which are towards the east of Selangor, were at a higher altitude, as shown in Figure 7b,c, the probability of them being converted to agricultural lands were minimal. Percentage of water cover in the 2001–2011 period can be attributed to construction of hydraulic structures and settlement ponds. Barren lands also decreased, but there was a rise in wetlands. In the 2011–2021 period, the changes in LULC experienced similar trends but at a substantially reduced rate. Forest and agricultural lands reduced, followed by a rise in developed and barren land. Wetlands saw marginal rise; however, water reduced significantly.

The main factors related to the increasing development land use at the expense of deteriorating the forest and agricultural covers can be attributed to urban expansion and growth in commercial agricultural [57]. The rapid urbanization has radically altered the natural environment and landscape patterns around the world, particularly in the twenty-first century [58]. The most important driving factors for urbanization are physical and social aspects, such as topography, population, and industrial growth [59]. Consequently, urban expansion is influenced more by economic growth than by population increase [60]. These expansions raise concerns regarding the effects of urbanization and disruption of land use patterns, which have effects on climate change, food security, and natural resources. The results obtained from the LULC classification indicate that the changes in the land use patterns are supported by the polices of the state [61–63].

Table 2. Changes in total area of different LULC classes between the years of 1991–2001, 2001–2011, and 2011–2021.

Periods LULC Classes	1991–2001 Area (Km^2)	2001–2011 Area (Km^2)	2011–2021 Area (Km^2)
Water	−1.40	37.84	6.90
Developed	296.19	874.81	96.64
Barren	143.90	4.95	10.43
Forest	−820.26	−250.70	−72.20
Agriculture	494.86	−681.52	−63.88
Wetlands	−113.29	14.62	22.11
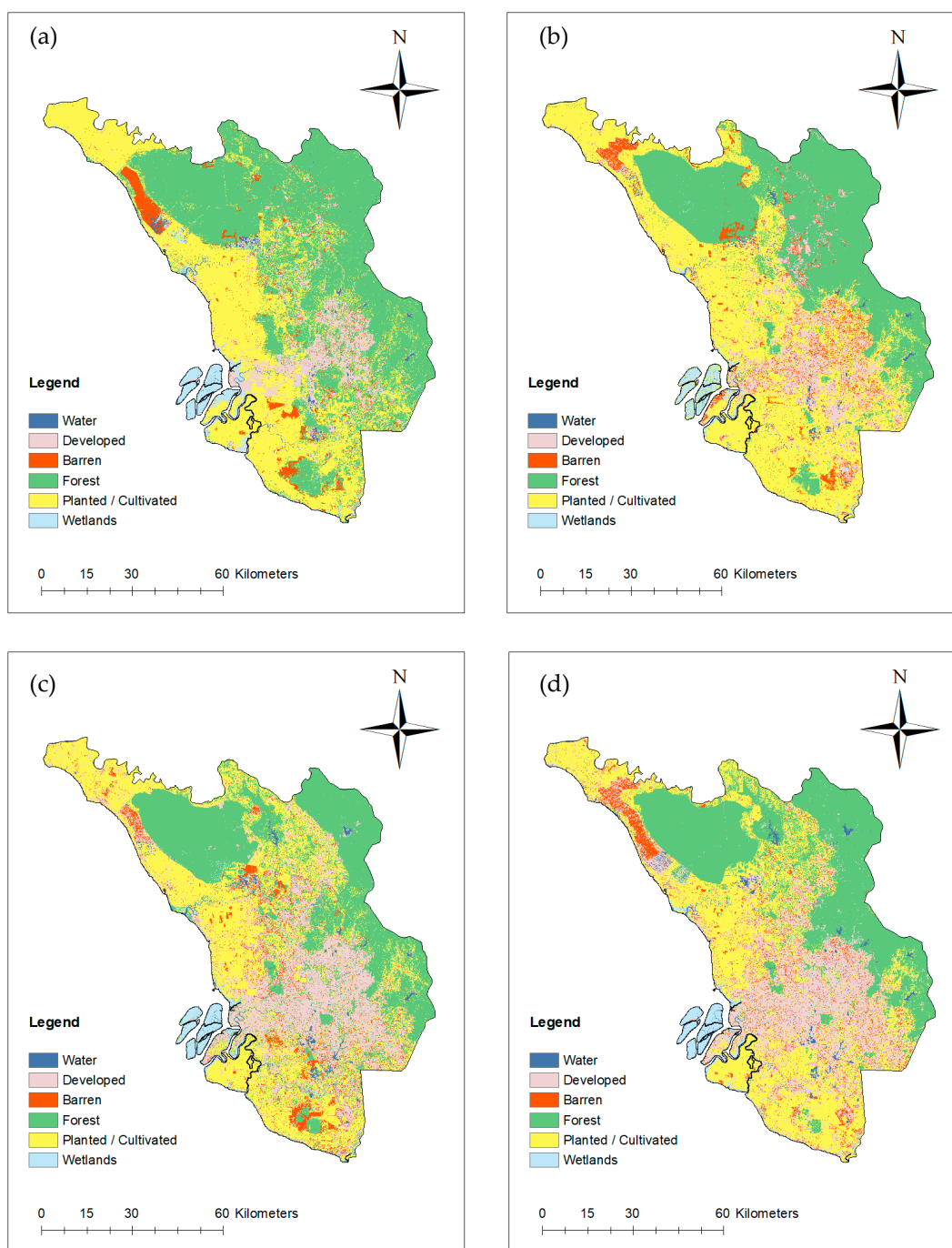
Figure 7. LULC classification maps of Selangor for (**a**) 1991, (**b**) 2001, (**c**) 2011, and (**d**) 2021.

3.2. Accuracy Assessment of LULC Maps

The accuracy of the classified LULC maps was assessed by comparing the land use classes with the satellite image (reference) ground truth data. The pixel-by-pixel accuracy assessment approach was undertaken based on which 150 random points were generated on the LULC maps of 1991, 2001, 2011, and 2021. The selected points were cross-referenced with the satellite images, as well as spatial maps of the study area. The selected points represent the various land use classes used for image classification. A confusion matrix was generated using the cross-referenced data to identify the degree of misclassified pixels by the image classification. Table 3 shows the percentage of accuracy based on the classified generated points (producer accuracy) and cross-referenced points (user accuracy) and the calculated overall accuracy and kappa coefficient. Multiple land use classification

trails were conducted to achieve the optimum accuracy, based on Anderson's classification scheme. An overall accuracy minimum of 85% is considered satisfactory of land use classification [28]. The analysis of the generated confusion matrix resulted in an overall accuracy of 96.7%, 94.0%, 94.0%, and 94.7% for the years 1991, 2001, 2011, and 2021, respectively. The corresponding kappa coefficient for the LULC maps of 1991, 2001, 2011, and 2021 was 0.96, 0.92, 0.92, and 0.93, respectively. The overall accuracies of the different land use classes are shown in Table 3. The overall accuracy of water and wetlands was observed to be relatively higher when compared with other land use classes as they were identified as clear pixels. On the other hand, barren lands were easily misclassified as the pixels were similar to developed lands. This was also observed between the classes of forest and agriculture. Areas with a greater concentration of mixed pixels belonging to different land use classes had a higher tendency of misclassification during the image classification process.

Table 3. Accuracy assessment of LULC maps from the years 1991 to 2021.

Accuracy Types	Year LULC	1991 %	2001 %	2011 %	2021 %
	Water	100.0	100.0	100.0	100.0
	Developed	95.8	97.1	98.0	98.0
Producer	Barren	77.8	80.0	58.3	81.8
Accuracy (%)	Forest	98.0	88.9	93.1	90.3
	Agriculture	97.9	98.0	97.6	94.6
	Wetlands	100.0	90.0	100.0	100.0
	Water	100.0	100.0	100.0	100.0
	Developed	92.0	94.4	90.6	96.2
User	Barren	87.5	88.9	87.5	90.0
Accuracy (%)	Forest	98.0	94.1	96.4	93.3
	Agriculture	97.9	94.1	95.3	92.1
	Wetlands	100.0	90.0	100.0	100.0
Overall Accuracy (%)		96.7	94.0	94.0	94.7
Kappa Coefficient		0.96	0.92	0.92	0.93

3.3. Transition Potential Modelling and Validation

The transitional changes undergone by the different land use classes between the years 2001 and 2011 are expressed as a confusion matrix in Table 4. These changes represent the distribution and conversion of individual land use class, as well as their nature of conversion. As observed from Table 4, some of the major transitions are agriculture to developed, forest to agriculture, and barren to developed and agricultural lands. These trends of land conversion and transition forms the basis of transition potential modelling for CA-ANN simulation. A changes map was created using the transition matrix. The changes map of 2001–2011 and spatial parameters (slope, aspect, and distance form roads) were considered as input parameters for training the ANN model.

Table 4. Accuracy assessment of LULC maps from the years 1991 to 2021.

Year				2011			
	Category	Water	Developed	Barren	Forest	Agriculture	Wetlands
	Water	0.997	0.00118	0.00046	0.00061	0.0006	0.0002
	Developed	0.017	0.731	0.086	0.054	0.1109	0.0015
	Barren	0.006	0.533	0.122	0.064	0.2737	0.0011
2001	Forest	0.002	0.050	0.024	0.748	0.1717	0.0040
	Agriculture	0.011	0.210	0.078	0.116	0.5740	0.0108
	Wetlands	0.015	0.045	0.009	0.075	0.0802	0.7751

The transition potential model (ANN) was validated by comparing the classified land use map of 2021 with the resulting simulated map of 2021 from the CA-ANN simula-

tion [57,64]. The comparison of the maps was evaluated based on the kappa coefficient value and percentage of correctness. The magnitude of correlation between the classified map and simulated map of 2021 is represented in the validation graph shown in Figure 8. The graph illustrates the degree of agreement between the different land use classes from the two maps. The land use classes in perfect agreement overlap each other, indicating that the land use pattern was simulated correctly, whereas deviance from the classified line denotes an inaccurate simulation of the land use pattern. The percentage of correctness for the simulation was 82.43%, and 0.72, 0.92, and 0.76 were the overall kappa, kappa histogram, and kappa location, respectively [57]. Based in the validated model, the CA-ANN simulation was executed to obtain the predicted land use maps of the years 2031, 2041, and 2051.
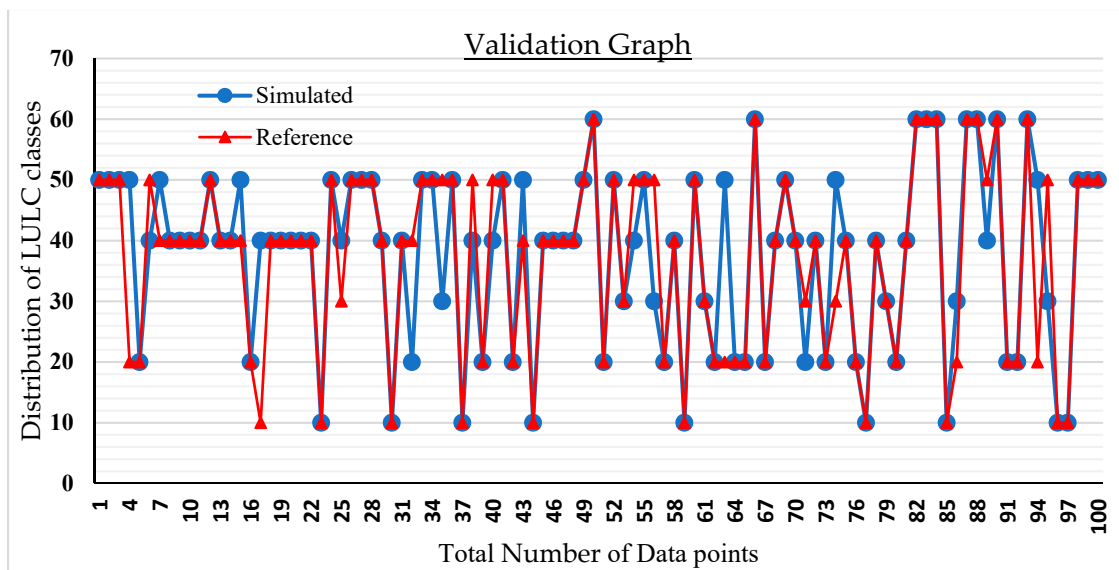
Figure 8. Validation graph illustrating the agreement between simulated and reference data points.

3.4. LULC Maps for the Predicted Years of 2031, 2041, and 2051

The CA-ANN simulation was performed to obtain the predicted LULC maps from the years 2031 to 2051. Figure 9 shows the predicted changes in different LULC classes from the years 2031 to 2051 in Selangor. Total area cover by different LULC classes and the percentage of cover for the years 2031, 2041, and 2051 are illustrated in Table 5. The observed outcomes elucidated the steady changes within the study period. A continued growth was noted in the developed land use pattern, where the area increased from 2874.31 Km^2 (35.23%) in 2031 to 3118.96 Km^2 (38.23%) in 2041, then to 3292.40 Km^2 (40.36%) in the year 2051. Due to the increasing rate of area covered by developed land, diminishing trends for forest and agricultural lands were observed in the simulated maps. Forest cover experiences a decline from 2536.46 Km^2 (31.09%) in 2031 to 2447.83 Km^2 (30.01%) in 2051. Similarly, agricultural cover also maintains its decreasing trend between the years 2031 and 2051 as the total percentage cover regresses from 27.51% to 23.78%, respectively. Water, barren, and wetlands experience a very minute change in their total area covered over the study period, as shown in Table 5. Water cover reduced slightly as the areas decreased from 85.14 Km^2 in 2031 to 81.80 Km^2 in 2051. Similarly, barren lands reduced from 284.25 Km^2 in 2031 to 266.75 Km^2 in 2051. Wetlands showed a drop in the percentage of area cover, reducing from 1.64% in 2031 to 1.58% in 2051.
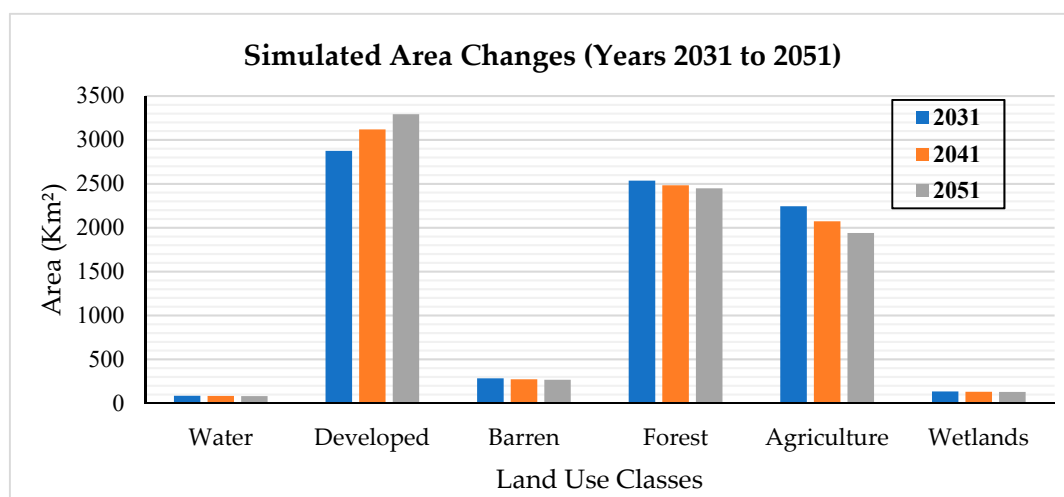
Figure 9. Predicted changes in different LULC classes in the years 2031, 2041, and 2051.

Table 5. Total area cover by different LULC classes and the percentage of cover for the years 2031, 2041, and 2051 in Selangor.

Years LULC Classes	2031 Area (Km^2)	%	2041 Area (Km^2)	%	2051 Area (Km^2)	%
Water	85.14	1.04	82.66	1.01	81.80	1.00
Developed	2874.31	35.23	3118.96	38.23	3292.40	40.36
Barren	284.25	3.48	272.03	3.33	266.75	3.27
Forest	2536.46	31.09	2482.07	30.42	2447.83	30.01
Agriculture	2244.04	27.51	2071.81	25.40	1940.11	23.78
Wetlands	133.80	1.64	130.48	1.60	129.11	1.58

Physical and socioeconomic factors had a substantial impact on landscape patterns during the study period, according to the observed outcomes. The geographical variables included in model calibration were chosen because of their significant relationship with LULC. Physical variables, such as geography and climate, are thought to be the most significant in promoting anthropogenic activity [65]. Socioeconomic factors, such as population and GDP, may have an impact on LULC change [66], while proximity factors, such as accessibility to highways, distance from the city center, and distance from the stream network, aid in determining the driving forces of the landscape pattern [67]. Areas with lower altitudes are often associated with rapid LULC changes, as the geography of these locations is more susceptible to anthropogenic activity. Since the slope towards the western regions of Selangor is comparably lower than that of other areas, the greatest changes happened in the plain areas of the state, particularly along the western shore. The mountainous, hilly, and forested areas of the north and east do not endure extensive fragmentation.

The outcomes of the simulated maps predict an increase in the expansion of commercial, industrial, and residential development at the cost of diminishing forest covers and agricultural lands, as shown in the simulated LULC maps for the years 2031, 2041, and 2051 in Figure 10. The driving causes of built-up expansion, according to several research, are population growth and economic development [46,68]. The natural ecosystem, water quality, and biodiversity are all harmed as the developed area grows [69]. Similarly, outcomes were noted by [57], where the prediction maps for the Great Bay area in China from 2030 to 2050 saw a rising trend in developed lands while agricultural lands continued decreasing. Yatoo et al. [64] also reported the rise of developed lands in the predicted LULC maps for the year 2027 in Ahmedabad, India. The findings also reflected a diminishing pattern of agricultural and water covered areas over the study period. The simulation of LULC maps from t 2031 to 2051 estimated a continuous surge in urban development in the state of Selangor.
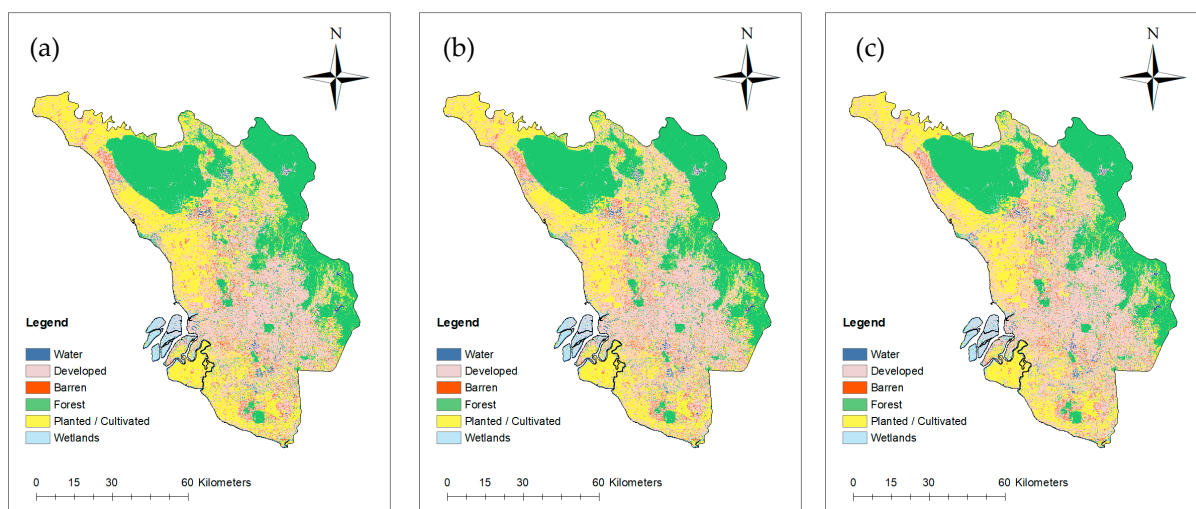
Figure 10. Simulated LULC maps of Selangor for: (**a**) 2031, (**b**) 2041, and (**c**) 2051.

4. Conclusions

The study identified the changes in the LULC patterns in the study area of Selangor, Malaysia, from 1991 to 2021. Land-use changes are mostly influenced by population and demand growth. To improve landscape planning and sustainable management, it is necessary to recognize harmful tendencies from the past years. Changing LULC patterns can also adversely affect the groundwater quality. For LULC classification, the support vector machine (SVM) offered accurate representations of land cover changes and related trends. Based on the observed outcomes of the classified maps, agricultural lands experienced a rapid increase from 35.82% in 1991 to 41.88% in 2001. A total of 9.13% of the agricultural area was reduced between 2001 and 2021. Developed lands experienced a 15.54% rise in the total percentage cover from 1991 to 2021. The driving factor for land-use change in Selangor was attributed to the rapid rate of urbanization and the conversion of agricultural lands for industrial expansions and urban settlements between 2011 and 2021. Forest covers experienced continuous degradation within the study time period as it diminished by 14.01%. Minimal changes were observed in the classes of water, barren, and wetlands. The analysis of the transition matrix signified the conversion of forest covers to agriculture and the expansion of developed lands upon agricultural lands. The CA-ANN-simulated maps of 2031, 2041, and 2051 also predicted the rise in developed areas and decline in forest and agricultural covers. Natural resources, ecology, and food security might all be jeopardized by severe changes in LULC, particularly due to urban expansion and agricultural fragmentation. The growing rate of urbanization and degradation of vegetation will greatly influence the quality of groundwater and exploitation of natural resources. Consequently, the spatiotemporal and prospective LULC simulation findings may aid decision-makers in analyzing LULC intensity changes and the effects of socioeconomic variables, as well as promoting environmental conservation and sustainable development plans. The influence of climatic changes (e.g., greenhouse gas emissions, land and water degradation, etc.), brought about by the rapid rate of industrial and urban expansion, as well as the extent of economic benefits to the state from industrial growth and land-use licensing, should be analyzed in future studies.

Author Contributions: Conceptualization, M.R.U.M.; data curation, M.F.B.; formal analysis, M.F.B. and M.R.U.M.; funding acquisition, M.R.U.M.; investigation, M.F.B. and M.R.U.M.; methodology, M.F.B.; project administration, M.R.U.M.; resources, M.R.U.M. and H.B.T.; supervision, M.R.U.M. and H.B.T.; validation, M.F.B.; writing—original draft, M.F.B.; writing—review and editing, M.R.U.M., I.B. and M.T.Z. All authors have read and agreed to the published version of the manuscript.

References

1. Houghton, R.A. The worldwide extent of land-use change. *BioScience* **1994**, *44*, 305–313. [CrossRef]
2. Hathout, S. The use of GIS for monitoring and predicting urban growth in East and West St Paul, Winnipeg, Manitoba, Canada. *J. Environ. Manag.* **2002**, *66*, 229–238. [CrossRef]
3. Fei, L.; Shuwen, Z.; Jiuchun, Y.; Liping, C.; Haijuan, Y.; Kun, B. Effects of land use change on ecosystem services value in West Jilin since the reform and opening of China. *Ecosyst. Serv.* **2018**, *31*, 12–20. [CrossRef]
4. López, E.; Bocco, G.; Mendoza, M.; Duhau, E. Predicting land-cover and land-use change in the urban fringe: A case in Morelia city, Mexico. *Landsc. Urban Plan.* **2001**, *55*, 271–285. [CrossRef]
5. Jat, M.K.; Garg, P.K.; Khare, D. Monitoring and modelling of urban sprawl using remote sensing and GIS techniques. *Int. J. Appl. Earth Obs. Geoinf.* **2008**, *10*, 26–43. [CrossRef]
6. Guerra, F.; Puig, H.; Chaume, R. The forest-savanna dynamics from multi-date Landsat-TM data in Sierra Parima, Venezuela. *Int. J. Remote. Sens.* **1998**, *19*, 2061–2075. [CrossRef]
7. Lipczynska-Kochany, E. Effect of climate change on humic substances and associated impacts on the quality of surface water and groundwater: A review. *Sci. Total. Environ.* **2018**, *640*, 1548–1565. [CrossRef] [PubMed]
8. Li, P.; Tian, R.; Xue, C.; Wu, J. Progress, opportunities, and key fields for groundwater quality research under the impacts of human activities in China with a special focus on western China. *Environ. Sci. Pollut. Res.* **2017**, *24*, 13224–13234. [CrossRef]
9. Rekha, P.N.; Gangadharan, R.; Ravichandran, P.; Dharshini, S.; Clarke, W.; Pillai, S.; Panigrahi, A.; Ponniah, A. Land-use/land-cover change dynamics and groundwater quality in and around shrimp farming area in coastal watershed, Cuddalore district, Tamil Nadu, India. *Curr. Sci.* **2017**, *113*, 1763–1770. [CrossRef]
10. Khan, R.; Jhariya, D. Assessment of land-use and land-cover change and its impact on groundwater quality using remote sensing and GIS techniques in Raipur City, Chhattisgarh, India. *J. Geol. Soc. India* **2018**, *92*, 59–66. [CrossRef]
11. He, S.; Wu, J. Hydrogeochemical characteristics, groundwater quality, and health risks from hexavalent chromium and nitrate in groundwater of Huanhe Formation in Wuqi county, northwest China. *Expo. Health* **2019**, *11*, 125–137. [CrossRef]
12. Sadeghi, A.; Galalizadeh, S.; Zehtabian, G.; Khosravi, H. Assessing the change of groundwater quality compared with land-use change and precipitation rate (Zrebar Lake's Basin). *Appl. Water Sci.* **2021**, *11*, 1–15. [CrossRef]
13. Singh, A. Review article digital change detection techniques using remotely-sensed data. *Int. J. Remote. Sens.* **1989**, *10*, 989–1003. [CrossRef]
14. Lu, D.; Mausel, P.; Brondizio, E.; Moran, E. Change detection techniques. *Int. J. Remote Sens.* **2004**, *25*, 2365–2401. [CrossRef]
15. Roy, A.; Inamdar, A.B. Multi-temporal Land Use Land Cover (LULC) change analysis of a dry semi-arid river basin in western India following a robust multi-sensor satellite image calibration strategy. *Heliyon* **2019**, *5*, e01478. [CrossRef]
16. Helmer, E.H.; Brown, S.; Cohen, W. Mapping montane tropical forest successional stage and land use with multi-date Landsat imagery. *Int. J. Remote Sens.* **2000**, *21*, 2163–2183. [CrossRef]
17. Hussain, M.; Chen, D.; Cheng, A.; Wei, H.; Stanley, D. Change detection from remotely sensed images: From pixel-based to object-based approaches. *ISPRS J. Photogramm. Remote Sens.* **2013**, *80*, 91–106. [CrossRef]
18. Singh, Y.; Ferrazzoli, P.; Rahmoune, R. Flood monitoring using microwave passive remote sensing (AMSR-E) in part of the Brahmaputra basin, India. *Int. J. Remote Sens.* **2013**, *34*, 4967–4985. [CrossRef]
19. Alexakis, D.; Agapiou, A.; Tzouvaras, M.; Themistocleous, K.; Neocleous, K.; Michaelides, S.; Hadjimitsis, D.G. Integrated use of GIS and remote sensing for monitoring landslides in transportation pavements: The case study of Paphos area in Cyprus. *Nat. Hazards* **2014**, *72*, 119–141. [CrossRef]
20. Yiridomoh, G.Y.; Appiah, D.O.; Owusu, V.; Bonye, S.Z. Women smallholder farmers off-farm adaptation strategies to climate variability in rural savannah, Ghana. *GeoJournal* **2021**, *86*, 2367–2385. [CrossRef]
21. Vibhute, A.D.; Gawali, B.W. Analysis and modeling of agricultural land use using remote sensing and geographic information system: A review. *Int. J. Eng. Res. Appl.* **2013**, *3*, 081–091.
22. Jiang, X.; Lu, D.; Moran, E.; Calvi, M.F.; Dutra, L.V.; Li, G. Examining impacts of the Belo Monte hydroelectric dam construction on land-cover changes using multitemporal Landsat imagery. *Appl. Geogr.* **2018**, *97*, 35–47. [CrossRef]

23. Hazarika, N.; Das, A.K.; Borah, S.B. Assessing land-use changes driven by river dynamics in chronically flood affected Upper Brahmaputra plains, India, using RS-GIS techniques. *Egypt. J. Remote Sens. Space Sci.* **2015**, *18*, 107–118. [CrossRef]

24. Iqbal, M.F.; Khan, I.A. Spatiotemporal land use land cover change analysis and erosion risk mapping of Azad Jammu and Kashmir, Pakistan. *Egypt. J. Remote Sens. Space Sci.* **2014**, *17*, 209–229. [CrossRef]

25. Mohamed, M.A. Monitoring of temporal and spatial changes of land use and land cover in metropolitan regions through remote sensing and GIS. *Nat. Resour.* **2017**, *08*, 353–369. [CrossRef]

26. El Gammal, E.A.; Salem, S.M.; El Gammal, A.E.A. Change detection studies on the world's biggest artificial lake (Lake Nasser, Egypt). *Egypt. J. Remote Sens. Space Sci.* **2010**, *13*, 89–99. [CrossRef]

27. Akinyemi, F.O. Land change in the central Albertine rift: Insights from analysis and mapping of land use-land cover change in north-western Rwanda. *Appl. Geogr.* **2017**, *87*, 127–138. [CrossRef]

28. Zeshan, M.T.; Mustafa, M.R.U.; Baig, M.F. Monitoring Land Use Changes and Their Future Prospects Using GIS and ANN-CA for Perak River Basin, Malaysia. *Water* **2021**, *13*, 2286. [CrossRef]

29. Mohammadi, A.; Shahabi, H.; Bin Ahmad, B. Land-Cover Change Detection in a Part of Cameron Highlands, Malaysia Using ETM+ Satellite Imagery and Support Vector Machine (SVM) Algorithm. *EnvironmentAsia* **2019**, *12*, 2.

30. Al-Najjar, H.A.; Kalantar, B.; Pradhan, B.; Saeidi, V.; Halin, A.A.; Ueda, N.; Mansor, S. Land cover classification from fused DSM and UAV images using convolutional neural networks. *Remote Sens.* **2019**, *11*, 1461. [CrossRef]

31. Seto, K.; Kaufmann, R. Using logit models to classify land cover and land-cover change from Landsat Thematic Mapper. *Int. J. Remote. Sens.* **2005**, *26*, 563–577. [CrossRef]

32. Richards, J.A.; Jia, X. Image classification methodologies. *Remote Sens. Digit. Image Anal. Introd.* **2006**, 295–332. Available online: https://scholar.google.com.hk/scholar?q=Image+classification+methodologies&hl=zh-CN&as_sdt=0&as_vis=1&oi=scholart (accessed on 10 November 2021).

33. Srivastava, P.K.; Han, D.; Rico-Ramirez, M.A.; Bray, M.; Islam, T. Selection of classification techniques for land use/land cover change investigation. *Adv. Space Res.* **2012**, *50*, 1250–1265. [CrossRef]

34. Cortes, C.; Vapnik, V. Support-vector networks. *Mach. Learn.* **1995**, *20*, 273–297. [CrossRef]

35. Vapnik, V. Statistical learning theory new york. *NY Wiley* **1998**, *1*, 2.

36. Talukdar, S.; Singha, P.; Mahato, S.; Praveen, B.; Rahman, A. Dynamics of ecosystem services (ESs) in response to land use land cover (LU/LC) changes in the lower Gangetic plain of India. *Ecol. Indic.* **2020**, *112*, 106121. [CrossRef]

37. Zhang, C.; Sargent, I.; Pan, X.; Li, H.; Gardiner, A.; Hare, J.; Atkinson, P.M. Joint Deep Learning for land cover and land use classification. *Remote. Sens. Environ.* **2019**, *221*, 173–187. [CrossRef]

38. Pal, M. Random forest classifier for remote sensing classification. *Int. J. Remote. Sens.* **2005**, *26*, 217–222. [CrossRef]

39. Civco, D.L. Artificial neural networks for land-cover classification and mapping. *Int. J. Geogr. Inf. Sci.* **1993**, *7*, 173–186. [CrossRef]

40. Carranza-García, M.; García-Gutiérrez, J.; Riquelme, J.C. A framework for evaluating land use and land cover classification using convolutional neural networks. *Remote Sens.* **2019**, *11*, 274. [CrossRef]

41. Ma, L.; Li, M.; Ma, X.; Cheng, L.; Du, P.; Liu, Y. A review of supervised object-based land-cover image classification. *ISPRS J. Photogramm. Remote Sens.* **2017**, *130*, 277–293. [CrossRef]

42. Mountrakis, G.; Im, J.; Ogole, C. Support vector machines in remote sensing: A review. *ISPRS J. Photogramm. Remote Sens.* **2011**, *66*, 247–259. [CrossRef]

43. Theobald, D.M.; Hobbs, N.T. Forecasting rural land-use change: A comparison of regression-and spatial transition-based models. *Geogr. Environ. Model.* **1998**, *2*, 65–82.

44. Pocewicz, A.; Nielsen-Pincus, M.; Goldberg, C.; Johnson, M.; Morgan, P.; Force, J.; Waits, L.; Vierling, L. Predicting land use change: Comparison of models based on landowner surveys and historical land cover trends. *Landsc. Ecol.* **2008**, *23*, 195–210. [CrossRef]

45. Lamchin, M.; Lee, W.-K.; Jeon, S.W.; Wang, S.W.; Lim, C.H.; Song, C.; Sung, M. Long-term trend and correlation between vegetation greenness and climate variables in Asia based on satellite data. *Sci. Total. Environ.* **2018**, *618*, 1089–1095. [CrossRef]

46. Reza, M.I.H. Southeast Asian Landscapes Are Facing Rapid Transition: A Study in the State of Selangor, Peninsular Malaysia. *Bull. Sci. Technol. Soc.* **2016**, *36*, 118–127. [CrossRef]

47. Abdullah, S.A.; Nakagoshi, N. Forest fragmentation and its correlation to human land use change in the state of Selangor, peninsular Malaysia. *For. Ecol. Manag.* **2007**, *241*, 39–48. [CrossRef]

48. Gao, J.; Liu, Y. Determination of land degradation causes in Tongyu County, Northeast China via land cover change detection. *Int. J. Appl. Earth Obs. Geoinf.* **2010**, *12*, 9–16. [CrossRef]

49. Shamsi, S.F. Integrating linear programming and analytical hierarchical processing in raster-GIS to optimize land use pattern at watershed level. *J. Appl. Sci. Environ. Manag.* **2010**, *14*, 2.

50. Hyandye, C.; Mandara, C.G.; Safari, J. GIS and logit regression model applications in land use/land cover change and distribution in Usangu catchment. *Am. J. Remote Sens.* **2015**, *3*, 6–16. [CrossRef]

51. Nedd, R.; Light, K.; Owens, M.; James, N.; Johnson, E.; Anandhi, A. A Synthesis of Land Use/Land Cover Studies: Definitions, Classification Systems, Meta-Studies, Challenges and Knowledge Gaps on a Global Landscape. *Land* **2021**, *10*, 994. [CrossRef]

52. Congalton, R.; Green, K. Thematic accuracy. *Assess. Accur. Remote Sens. Data Princ. Pr.* **2009**, *4*, 55–61.

53. Laliberte, A.S.; Rango, A.; Havstad, K.M.; Paris, J.F.; Beck, R.F.; McNeely, R.; Gonzalez, A.L. Object-oriented image analysis for mapping shrub encroachment from 1937 to 2003 in southern New Mexico. *Remote Sens. Environ.* **2004**, *93*, 198–210. [CrossRef]

54. Rahman, M.T.U.; Tabassum, F.; Rasheduzzaman, M.; Saba, H.; Sarkar, L.; Ferdous, J.; Uddin, S.Z.; Islam, A.Z. Temporal dynamics of land use/land cover change and its prediction using CA-ANN model for southwestern coastal Bangladesh. *Environ. Monit. Assess.* **2017**, *189*, 1–18. [CrossRef] [PubMed]

55. El-Tantawi, A.M.; Bao, A.; Chang, C.; Liu, Y. Monitoring and predicting land use/cover changes in the Aksu-Tarim River Basin, Xinjiang-China (1990–2030). *Environ. Monit. Assess.* **2019**, *191*, 1–18. [CrossRef]

56. Memarian, H.; Balasundram, S.K.; Talib, J.B.; Sung, C.T.B.; Sood, A.M.; Abbaspour, K. Validation of CA-Markov for simulation of land use and cover change in the Langat Basin, Malaysia. *J. Geogr. Inf. Syst.* **2012**, *04*, 542–554. [CrossRef]

57. Abbas, Z.; Yang, G.; Zhong, Y.; Zhao, Y. Spatiotemporal Change Analysis and Future Scenario of LULC Using the CA-ANN Approach: A Case Study of the Greater Bay Area, China. *Land* **2021**, *10*, 584. [CrossRef]

58. Seto, K.C.; Kaufmann, R.K. Modeling the drivers of urban land use change in the Pearl River Delta, China: Integrating remote sensing with socioeconomic data. *Land Econ.* **2003**, *79*, 106–121. [CrossRef]

59. Yin, J.; Yin, Z.; Zhong, H.; Xu, S.; Hu, X.; Wang, J.; Wu, J. Monitoring urban expansion and land use/land cover changes of Shanghai metropolitan area during the transitional economy (1979–2009) in China. *Environ. Monit. Assess.* **2011**, *177*, 609–621. [CrossRef]

60. Guangjin, T.; Xinliang, X.; Xiaojuan, L.; Lingqiang, K. The comparison and modeling of the driving factors of urban expansion for thirty-five big cities in the three regions in China. *Adv. Meteorol.* **2016**, *2016*, 1–9. [CrossRef]

61. Abdullah, J. City competitiveness and urban sprawl: Their implications to socio-economic and cultural life in Malaysian cities. *Procedia-Soc. Behav. Sci.* **2012**, *50*, 20–29. [CrossRef]

62. Olaniyi, A.; Abdullah, A.; Ramli, M.; Sood, A. Agricultural land use in Malaysia: An historical overview and implications for food security. *Bulg. J. Agric. Sci.* **2013**, *19*, 60–69.

63. Golam Hassan, A.A.; Ngah, I.; Applanaidu, S.D. Agricultural Transformation in Malaysia: The Role of Smallholders And Area Development. *Development* **2018**, *15*, 2.

64. Yatoo, S.A.; Sahu, P.; Kalubarme, M.H.; Kansara, B.B. Monitoring land use changes and its future prospects using cellular automata simulation and artificial neural network for Ahmedabad city, India. *GeoJournal* **2020**, *85*, 1–22. [CrossRef]

65. Wu, Q.; Li, H.-q.; Wang, R.-s.; Paulussen, J.; He, Y.; Wang, M.; Wang, B.-h.; Wang, Z. Monitoring and predicting land use change in Beijing using remote sensing and GIS. *Landsc. Urban Plan.* **2006**, *78*, 322–333. [CrossRef]

66. Li, X.; Wang, Y.; Li, J.; Lei, B. Physical and Socioeconomic Driving Forces of Land-Use and Land-Cover Changes: A Case Study of Wuhan City, China. *Discret. Dyn. Nat. Soc.* **2016**, *2016*, 8061069. [CrossRef]

67. Serneels, S.; Lambin, E.F. Proximate causes of land-use change in Narok District, Kenya: A spatial statistical model. *Agric. Ecosyst. Environ.* **2001**, *85*, 65–81. [CrossRef]

68. Wu, R.; Li, Z.; Wang, S. The varying driving forces of urban land expansion in China: Insights from a spatial-temporal analysis. *Sci. Total. Environ.* **2021**, *766*, 142591. [CrossRef]

69. Seto, K.C.; Güneralp, B.; Hutyra, L.R. Global forecasts of urban expansion to 2030 and direct impacts on biodiversity and carbon pools. *Proc. Natl. Acad. Sci. USA* **2012**, *109*, 16083–16088. [CrossRef] [PubMed]